Flexibility of Interdomain Contacts Revealed by Topological Isomers of Bivalent Consolidated Ligands to the Dual Src Homology Domain SH(32) of Abelson[†,‡]

Qinghong Xu,[§,∥,⊥] Jie Zheng,[§,⊥] Rong Xu,[§] George Barany,[∥] and David Cowburn*,[§]

The Rockefeller University, 1230 York Avenue, New York, New York 10021, and Department of Chemistry, University of Minnesota, 207 Pleasant Street S.E., Minneapolis, Minnesota 55455

Received November 18, 1998; Revised Manuscript Received January 13, 1999

ABSTRACT: Src homology (SH)2 and SH3 domains are found in a variety of proteins involved in the control of cellular signaling and architecture. The possible interrelationships between domains are not easily investigated, even though several cases of multiple domain-containing constructs have been studied structurally. As a complement to direct structural methods, we have developed consolidated ligands and tested their binding to the Abl SH(32) complex. Consolidated ligands combine in the same molecule peptide sequences recognized by SH2 and SH3 domains, i.e., Pro-Val-pTyr-Glu-Asn-Val and Pro-Pro-Ala-Tyr-Pro-Pro-Pro-Pro-Val-Pro, respectively; these are joined by oligoglycyl linkers. Four types of ligands were chemically synthesized, representing all the possible relative orientations of ligands. Their affinities were found to vary with binding portion topologies and linker lengths. Two of these types were shown to bind to both SH2 and SH3 dual domains with high affinities and specificities, showing increases of one order of magnitude, as compared to the most strongly bound monovalent equivalent. These results suggest that the relative orientation of SH2 and SH3 in Abl SH(32) is not fixed, and this synthetic approach may be generally useful for determining the structures of ligated complexes and for developing reagents with high affinities and specificities.

Many proteins involved in intracellular signal transduction contain multiple domains, as do proteins in other functional classes (*1*). These domains, especially SH2,[1] SH3, and PH domains (*2*−*4*), can fold into compact structures themselves and display the appropriate partial function of the whole protein. The interrelationships between these domains in a whole protein are likely to be involved in the integrated biological function, and are of considerable significance (*5*−*10*). Recently, we demonstrated that a series of synthetic ligands can interact simultaneously with the SH2 and SH3 domains of Abelson kinase in a SH(32) dual domain construct (*11*). These consolidated ligands have enhanced affinity and specificity compared to their monovalent equivalents. In this paper, we extend the earlier observations to the complete treatment of the different possible topologies of combining the linear epitopes involved; we show the enhancement of affinities in two of these topological series of four ligands, and show that this arises from the formation of 1:1 complexes. These results are consistent only with a highly flexible picture of the range of SH3 and SH2 interdomain relationships, in contrast to the "snapshot" seen in crystallographic studies of similar complexes (*5*, *7*). Since the flexibility of these domains is significant in the modulation of Src family enzymatic activity (*12*) or the interplay of subdomains in adapters (*13*, *14*), it is important to understand what the range and role of such flexibility may be in the control of protein tyrosine kinases' self-inhibition and processive phosphorylation (*15*).

SH2 domains recognize motifs that include key phosphotyrosine residues (*16*), while SH3 domains recognize sequence with multiple proline residues. The two domains are frequently found together in the same protein, for example, in the Abelson kinase (Abl). The technical limitations to current structural approaches to multiple domain proteins led to experiments involving designed ligands, which can be used to modify the activities of those proteins and to analyze the structures of the ligand-binding domains by simultaneous binding to multiple sites.

[†] This work was supported by National Institutes of Health Grants GM-47021 and GM-525405 (to D.C.) and GM-42722 and GM-51628 (to G.B.). Q.X. is the C. H. Li Memorial Fund Fellow.

[‡] Portions of this work were reported in preliminary form: Xu, Q., Zheng, J., Barany, G., and Cowburn, D. (1999) in *Peptides: Chemistry, Structure and Biology: Proceedings of the Fifteenth American Peptide Symposium*, Nashville, TN, June 14−19, 1997 (Tam, J. P., and Kaumaya, P. T. P., Eds.) pp 156−157, Kluwer, Dordercht, The Netherlands.

* To whom correspondence should be addressed. Telephone: (212) 327-8270. Fax: (212) 327-7566. E-mail: cowburn@rockvax.rockefeller.edu.

[§] The Rockefeller University.

[∥] University of Minnesota.

[⊥] Both authors contributed equally to this work.

[1] Amino acid symbols denote the L-configuration, and abbreviations for amino acids and peptides follow rules of the IUPAC−IUB Commission of Biochemical Nomenclature [(1972) *J. Biol. Chem. 247*, 977−983]. Other abbreviations: SH2, Src homology type 2; SH3, Src homology type 3; PH, pleckstrin homology; BOP, benzotriazol-1-yl-*N*-oxytris(dimethylamino)phosphonium hexafluorophosphate; Dde, 1-(4,4-dimethyl-2,6-dioxocyclohexylidene)ethyl; DIEA, *N*,*N*-diisopropylethylamine; Fmoc, *N*-(9-fluorenyl)methoxycarbonyl; HATU, *N*-[(dimethylamino)-1*H*-1,2,3-triazolo[4,5-*b*]pyridin-1-yl-methylene]-*N*-methylmethanaminium hexafluorophosphate *N*-oxide; HBTU, *N*-[(1*H*-benzotriazol-1-yl)(dimethylamino)methylene]-*N*-methylmethanaminium hexafluorophosphate *N*-oxide; HOAt, 1-hydroxy-7-azabenzotriazole; HOBt, 1-hydroxybenzotriazole; NMM, *N*-methylmorpholine; PAL, 5-[[(4-amino)-methyl]-3,5-dimethoxyphenoxy]valeric acid; PEG-PS, polyethylene glycol-polystyrene. All solvent ratios are volume/volume unless stated otherwise.

10.1021/bi982744j CCC: $18.00 © 1999 American Chemical Society
Published on Web 03/05/1999

Since both bound ligands have a fixed orientation, only those consolidated ligands which have a correct linkage, in terms of both length and topology, will fit the relative orientations of the SH3 and SH2 domains in the SH(32) construct simultaneously. The topology of the first group of enhanced-affinity consolidated (type A) ligands was designed on the basis of the orientation of SH(32) seen in the crystal structure of Lck (*5*) and is consistent with earlier studies in solution of Abl SH(32) (*6*). However, this type of consolidated ligand will not fit in the apparent conformations of SH(32) as seen in the crystal structure of Abl SH(32) (*7*) or of Grb-2 (*13*). To elucidate the possible existence of alternative orientations of SH3 and SH2 in the complex, we synthesized additional consolidated ligands with alternative topologies and linker lengths, and showed the flexibility of these two domains.

MATERIALS AND METHODS

General. Some of the materials and general synthetic and analytical procedures have been described in earlier publications (*17*−*19*). Fmoc-Tyr(PO_3H_2)-OH and Fmoc-Lys(Dde)-OH were from Novabiochem (San Diego, CA). Other protected Fmoc-amino acid derivatives, as well as coupling reagents and resins for peptide synthesis, were from the Biosearch Division of PerSeptive Biosystems (Framingham, MA), Bachem Bioscience (Philadelphia, PA), or Advanced Chemtech (Louisville, KY). Piperidine, trifluoroacetic acid (TFA), *N*,*N*-diisopropylethylamine (DIEA), and 1-hydroxybenzotriazole (HOBt) were from Fisher (Pittsburgh, PA). *N*,*N*′-Diisopropylcarbodiimide (DIPCDI) was from Aldrich (Milwaukee, WI).

Analytical HPLC was performed using a Vydac analytical C-18 reversed-phase column (218TP54; 5 μm, 300 Å; 0.46 cm × 25 cm) on a Beckman system configured with two model 112 pumps and a model 165 variable-wavelength detector controlled from an IBM computer with Beckman System Gold software. Peptide samples were chromatographed at 1.2 mL/min with 0.1% aqueous TFA/CH_3CN (10:0 for 10 min and then a gradient to 2:3 over the course of the next 25 min), with detection at 220 nm. Semipreparative HPLC to purify crude peptide products obtained after cleavage was performed on a Vydac semipreparative C-18 reversed-phase column (218TP1010; 10 μm, 300 Å; 1.0 cm × 25 cm) on a Waters Deltaprep system using manual injection (3 mL, ∼20 mg of peptide per run) and elution at a flow rate of 5 mL/min using 0.1% aqueous TFA/CH_3CN, (19:1 to 1:1 over the course of 55 min), with detection at 220 nm. Fractions with the correct peptide were pooled and lyophilized to provide white powders. Isolated yields were typically 20−40% with purities of ≥93% as judged by analytical HPLC. Amino acid analyses were performed on a Beckman 6300 Analyzer with a sulfated polystyrene cation-exchange column (0.4 cm × 21 cm). Free peptides were hydrolyzed with 6 N aqueous HCl at 110 °C for 24 h. Electrospray mass spectrometry (ESMS) was performed on a PESciex API III triple-quadrupole mass spectrometer equipped with an ion-spray interface. The following parameters were used: ion-spray voltage of 5000 V, interface temperature of 55 °C, potential on the first quadrupole of 30 V, and an orifice voltage from 55 to 80 V. The flow rates for the curtain gas (N_2) and the nebulizer gas (ultrapure air) were set at 0.8−1.0 L/min. Molecular masses were calculated with the Sciex Macspec 3.22 program.

Syntheses of Type A Ligands. The branched orientations of these peptides were achieved by solid-phase synthesis as outlined (Figure 1), according to experimental details published elsewhere (*19*). In brief, syntheses started with Fmoc-PAL-PEG-PS resin (∼600 mg, 0.16 mmol/g) and repetitive steps were carried out either manually or on a continuous flow PerSeptive BioSystems 9050 instrument. Fmoc removal was performed with piperidine/DMF (1:4, 2 + 8 min), and couplings were achieved by combining solid N^{α}-Fmoc-amino acid (4 equiv, 0.5 M), HOBt (4 equiv, 0.5 M), BOP (4 equiv, 0.5 M), and NMM (8 equiv, 1.0 M) in DMF for 1 h. However, incorporation of Asn was achieved by using N^{α}-Fmoc-Asn-OPfp/HOBt (4 equiv each) in DMF for 1 h. NMM was substituted with DIEA at the step where N^{α}-Fmoc-Tyr(PO_3H_2)-OH was coupled, and in all subsequent couplings. Dde removal to introduce a branch point involved treatment with anhydrous hydrazine hydrate/DMF (1:49, 6 × 5 min). After chain assembly was complete, the final deprotection and cleavage steps were carried out using reagent K (35:2:2:2:1 TFA/phenol/H_2O/thioanisole/1,2-ethanedithiol) (*20*) for 3 h at 25 °C. Purification and characterization were as already described (*19*).

Model Studies of Fragment Coupling: Addition of H-Pro-Ala-NH_2 to Glutaric Anhydride-Modified Ala-Phe-PAL Resin. Solid-phase syntheses started from Fmoc-PAL-PEG-PS resin (100 mg, 0.16 mmol/g) using BOP/HOBt/NMM protocols as described above. The dipeptide H-Pro-Ala-NH_2 was isolated after cleavage with reagent R (90:5:3:2 TFA/thioanisole/1,2-ethanedithiol/anisole) (*17*). The free amine of Ala-Phe-PAL resin (swollen in CH_2Cl_2) was acylated by adding glutaric anhydride (18 mg, 10 equiv)/triethylamine (46 μL, 20 equiv) in CH_2Cl_2 (0.1 mL) for 30 min, followed by washing with CH_2Cl_2 (5 × 2 min) and DMF (5 × 2 min). The pendant ω-carboxyl peptide resin (swollen in DMF) was preactivated in situ by addition of different coupling reagents, listed in Table 1, in DMF (0.2 mL) for 10 min, and then free peptide H-Pro-Ala-NH_2 (5.8 mg, 2 equiv) dissolved in DMF (20 μL) was added to the activated peptide resin. After coupling for 6 h, the peptide resins were washed with DMF (5 × 2 min) and CH_2Cl_2 (5 × 2 min), followed by final cleavage with reagent R as described above. Analytical HPLC using a C-18 reversed-phase column, eluted at a flow rate of 1.2 mL/min with 0.1% aqueous TFA/CH_3CN (10:0 for 8 min, and then a gradient to 17:3 over the next 12 min), with detection at 220 nm, showed the acylated Ala-Phe-NH_2 at 17.1 min and the expected product model tetrapeptide at 17.5 min (characterized further by amino acid analysis and ESMS, calcd 516.2, found 517.0 [MH^+]).

Syntheses of Type B Ligands via Fragment Coupling. These syntheses were carried out essentially as already outlined, including direct incorporation of the N^{α}-Fmoc-Tyr-(PO_3H_2)-OH derivative. The 2BP-1 (SH2 binding ligand) sequence and the oligoglycyl spacer were assembled on PAL-PEG-PS (200 mg, 0.16 mmol/g, swelling in CH_2Cl_2), followed by acylation of the free amine by addition of glutaric anhydride (36 mg, 10 equiv)/Et_3N (92 μL, 20 equiv) in CH_2Cl_2 (0.2 mL) for 30 min. The pendant ω-carboxyl was coupled with the 3BP-2 amide (SH3 binding ligand) sequence (33 mg, 2 equiv) that had been made separately

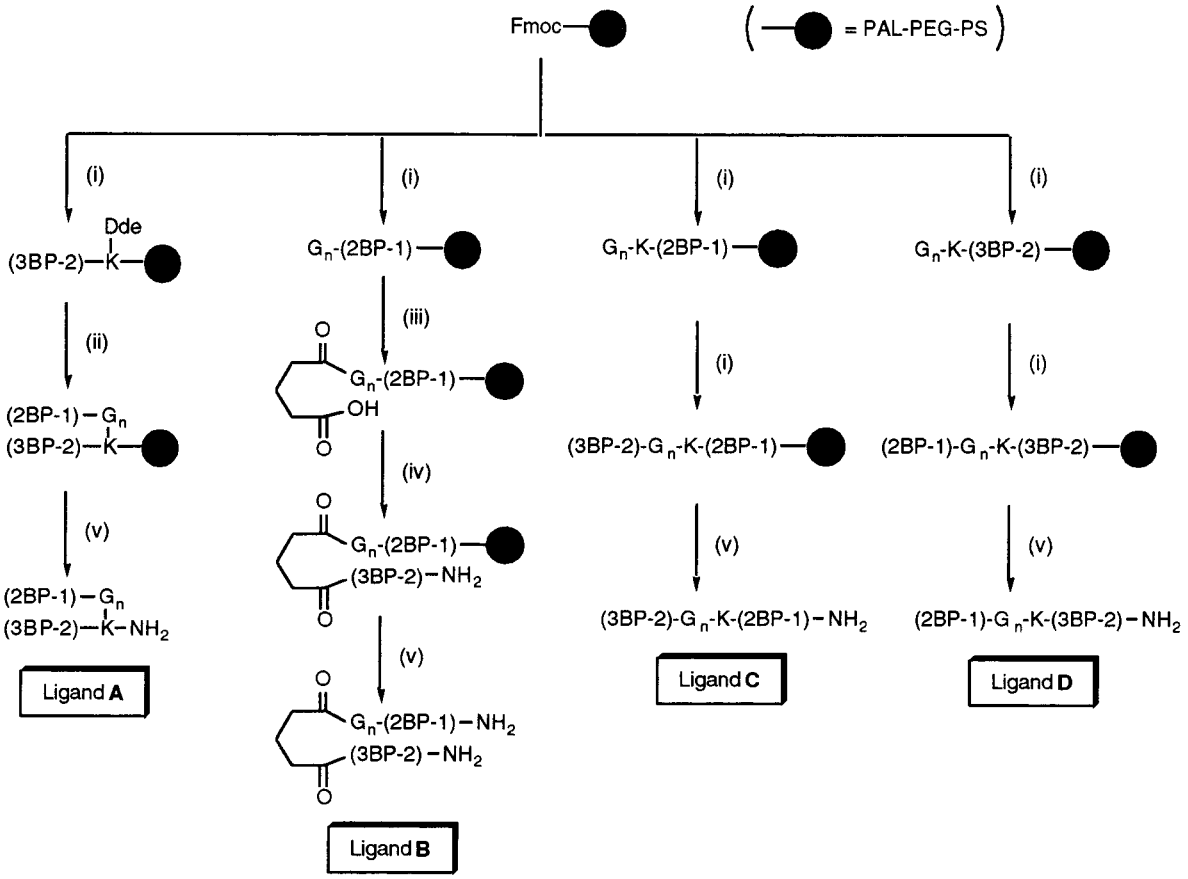

FIGURE 1: Solid-phase synthesis of ligands. (i) Incorporation of residues from the indicated structure by Fmoc chemistry with the BOP/HOBt/NMM protocol. NMM was replaced by DIEA starting with the step for incorporation of Fmoc-Tyr(PO_3H_2)-OH. (ii) Removal of Dde by hydrazine hydrate/DMF (1:49 v/v, 6 × 5 min), followed by G_n and 2BP-1 assembly. (iii) Glutaric anhydride/Et_3N (10:20) in CH_2Cl_2 (30 min). (iv) Coupling of (3BP-2)-NH_2 (2 equiv) by HATU/HOAt/NMM (2:2:4) in DMF (6 h). (v) Cleavage from polymer support by reagent K (35:2:2:2:1 TFA/phenol/H_2O/thioanisole/1,2-ethanedithiol) for 2 h. The sequence of 2BP-1 is PVY*ENV (Y* is phosphotyrosine); the sequence of 3BP-2 is PPAYPPPPVP, and NH_2 refers to carboxamide function at the C-terminus.

Table 1: Model Coupling Yields as a Function of the Reagents Used[a]

	coupling conditions	% product
1	BOP/HOBt/NMM (2:2:4)	47
2	HBTU/HOBt/NMM (2:2:4)	80
3	HATU/HOAt/NMM (2:2:4)	94
4	DIPCDI/HOBt (2:2)	3
5	DIPCDI/HOAt (2:2)	6

[a] H-Pro-Ala-NH_2 (2 equiv) and $HO_2C(CH_2)_3(C{=}O)$-Ala-Phe-PAL-PEG-PS (1 equiv) for 6 h (further details in Materials and Methods).

on PAL-PEG-PS, cleaved, and purified (peptide was characterized by ESMS, calcd 1029.8, found 1030.2 [MH^+]), in the presence of HATU (24.3 mg, 2 equiv)/HOAt (8.9 mg, 2 equiv)/NMM (14.4 μL, 4 equiv) in DMF (0.25 mL) for 6 h (characterized by ESMS, for $n = 6$, calcd 2265.1, found 2266.7 [MH^+]; for $n = 7$, calcd 2322.1, found 2323.8 [MH^+]).

Syntheses of Type C and D Ligands by Stepwise SPPS. These syntheses were carried out by procedures already outlined. For the newly synthesized type C ligands, the ESMS data were as follows: for $n = 6$, calcd 2281.1, found 2281.8 [MH^+]; for $n = 7$, calcd 2338.1, found 2338.8 [MH^+]; and for $n = 8$, calcd 2395.1, found 2394.9 [MH^+]. The single representative of type D was reported previously (*19*).

Syntheses of Control Peptides (Figure 2 Legend). An analogue of type A ligands ($n = 6$), in which the lysine side chain link is adjacent to the 2BP-1 segment, was synthesized by the general procedure, including direct incorporation of C-terminal lysine as its N^{α}-Fmoc, N^{ϵ}-Dde derivative, and incorporation of N^{α}-Fmoc-Tyr(PO_3H_2)-OH. The characterization of this peptide was reported previously (*19*). An analogue of type C ligands, in which the lysine is replaced by another glycine, was synthesized essentially as described above: ESMS calcd 2210.0, found 2210.9 [MH^+].

Affinity Measurements. Concentrations of proteins and peptides were determined by UV absorbance at 264 nm, using values of 1752 for phosphotyrosyl and 840 for tyrosyl for mean residue absorption coefficients. Affinities were measured by intrinsic fluorescence quenching using a Perkin-Elmer 760-40 apparatus, with excitation at 290 nm, and emission at 345 nm, with effective bandwidths of 2 and 17 nm, respectively. The changes of fluorescence observed are apparently additive for the occupancy of the SH2 and SH3 sites. The SH3 site has an apparent level of quenching that is about 4-fold greater than that for the SH2 site in the individual domains. The sample compartment was maintained at 18 °C, and a minimagnetic stirrer was used for continuous mixing. Titration of SH domains was accomplished by making appropriate sequential additions from the peptide stock solution to the domain(s) in a 1 cm square quartz cell. Fluorescence was recorded 2 min after each addition. One milliliter of a protein solution [140 mM NaCl and 5 mM phosphate (pH 7.3)] with 1 mM DTT was used.

Ligands		A	B	C	D
Linker -G_n- (nM)	G_3		15,290		
	G_5	503 (III)			
	G_6	249 (IV)	11,900	403	22,100 (V)
	G_7	327 (VI)	19,280	190	
	G_8	389 (VII)		219	
Binding Subdomains		SH2 + SH3	SH2	SH2 + SH3	SH2

2BP-1 Linker 3BP-2

FIGURE 2: Affinities, in nanomolar, of ligands for SH(32) of Abl. The structures of constituent ligands, termed 2BP-1 (PVY*ENV) and 3BP-2 (PPAYPPPPVP), were known from biological screening of either chemically synthesized model peptides or hybrid proteins that included these sequences. Our early studies have shown the design consideration for these consolidated ligands which have enhanced affinities and specificities. Ligands were synthesized as illustrated in Figure 1; the type A, C, and D ligands include lysine at the C-terminus of the G_n linker. The affinity assay has been described previously (further details in Materials and Methods). The compounds in columns A and D were previously described and assayed (*11*), and their numbering in that reference is shown in braces. The linker is not symmetric, so there are additional questions concerning the role that the positioning and stereochemistry of the inserted lysine might play. For type C, the compound (3BP-2)-G_7-(2BP-1)-NH_2 had an affinity (750 nM) similar to that of the lysine-containing (3BP-2)-G_6K-(2BP-1)-NH_2 (403 nM; this figure type C, G_6). However, the type A compound in which the 2BP-1 segment is attached to the α-amine of lysine and the 3BP-2 fragment is attached to the G_6 spacer on the lysine ϵ-amine side chain (compound **XI**; *11*) has an affinity of 3200 nM, about 10-fold lower than that of its analogue reported in the figure (e.g., type A, G_6; 249 nM). The stereocenter in lysine may not permit access to the 2BP segment needed for binding as efficiently as a G residue. Synthetic strategies for symmetric linkers are currently being studied.

Protein concentrations were approximately 500 nM, determined accurately by absorption prior to dilution. Data were analyzed using the program Origin (Microcal Software, Inc. 4.0) to fit the equation

$$[\text{total}] - [\text{ligand}] = [K_d(F - F_0) + [F_{max} - (F - F_0)](F - F_0)([\text{total}] - [\text{protein}])/F_{max}]/[F_{max} - (F - F_0)]$$

where F is the observed fluorescence quenching at the total ligand concentration [total], F_{max} is the level of quenching of protein saturated with ligand, and F_0 is the fluorescence without ligand. K_d, F_{max}, and F_0 are treated as fitted parameters.

NMR Spectroscopy. NMR spectra were obtained on Bruker DMX 500 MHz NMR spectrometers, at 35 °C, in a phosphate buffer [200 mM NaCl, 8 mM sodium phosphate, 2.7 mM KCl, and 1.4 mM potassium phosphate (pH 7.2)], with 0.02% sodium azide and 10% D_2O. The construct used for NMR substituted an easily oxidized cysteine in SH3, has nongenomic N- and C-terminal sequences slightly different from the constructs used previously (*6*, *11*), and has the sequence gspggsLFVALYDFVASGDNTLSITKGEKLRVL-GYNHNGEWAEAQTKNGQGWVPSNYIT-PVGCLEKHSWYHGPVSRNAAEYLLSSGINGSFLV-RESESSPGQRSISLRYEGRVYHYRINTAS-DGKLYVSSESRFNTLAELVHHHSTVADG-LITTLHYPAPKRgihrd, where the lowercase letters represent those amino acids introduced by the expression system used. This SH(32) construct had the same affinities to the ligands of reference (*11*), within experimental error, and is assumed to be functionally identical to the earlier construct throughout this discussion. Ligand titrations were performed by the addition of small volumes of peptide in buffer to the protein NMR sample, and are not corrected in intensity for dilution effects. Spectra observed were typically HSQC spectra with ^{1}H and ^{15}N sweep widths of 14 and 50 ppm, respectively (Figure 3).

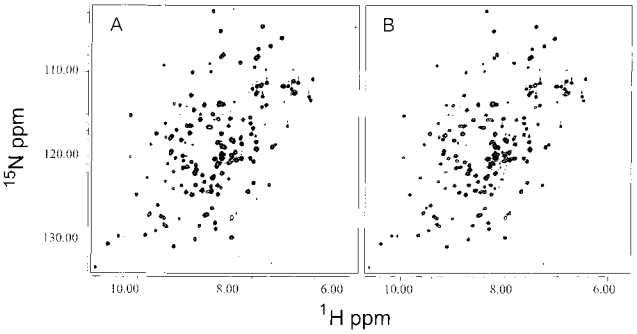

FIGURE 3: NMR spectroscopy of Abl SH(32) with binding ligands. 500 MHz ^{1}H{^{15}N} NMR spectra of Abl SH(32) in complex (A) with a type A ligand ($n = 6$) and (B) with a type C ligand ($n = 7$). The resolution is 0.007 ppm in the ^{1}H dimension and 0.1 ppm in the ^{15}N dimension.

Molecular Modeling and Display. Structures [PDB codes 1LCK (*5*), 1GRI (*13*), 2ABL (*7*), 1FMK (*9*), 2HCK (*8*), 1AB2 (*21*), 1AB3 (*22*), and 2AB3 (*6*)] were superimposed on one or both domains using the common secondary structural (Figure 4) heavy atoms of the backbone with INSIGHT II (Molecular Simulations Inc.). Structures are displayed using Insight, or SETOR (*23*).

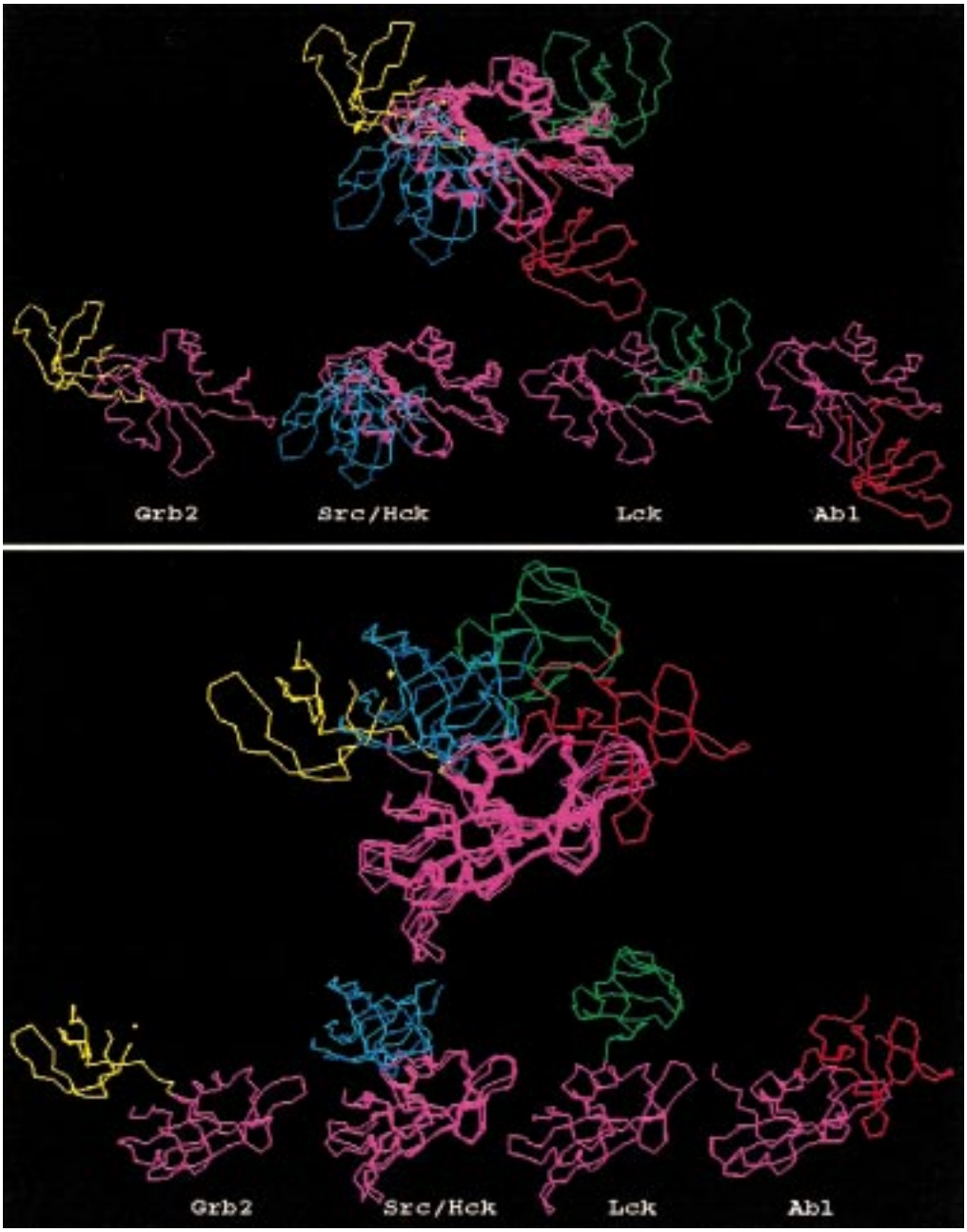

FIGURE 4: Computer modeling and display of SH(32) dual domains in various proteins. The crystal structures of the SH2 of the SH(32) segments of Grb2, Src/Hck, Lck, and Abl are superimposed, on the basis of the backbone alignment of their SH2 domain (in magenta), and SH3 domains are shown in a different color for different proteins. The display illustrates the wide variety of conformational orientations in the SH(32) dual domain.

Isothermal Titration Calorimetry. ITC studies were performed using the Omega instrument from MicroCal Inc. (Northampton, MA) (*24*). In a typical titration, the peptide was added over 20 injections (of 6 μL) to Abl SH(32) that was present in the isothermal calorimeter cell at 20 °C. The buffer in which the titrations were performed was 50 mM potassium phosphate (pH 7.2). Heats of dilution for both reactants with buffer solution were determined in separate experiments. The total measured heats were corrected for these heats of dilution prior to data analysis. Titration curves were fit using the ORIGIN software (MicroCal Inc.). Protein concentrations were determined by measuring A_{280} (ϵ = 30 000) and peptide concentrations by measuring A_{264} (ϵ = 2592) using the extinction coefficient that had been checked by comparison with the results from quantitative amino acid analysis.

RESULTS AND DISCUSSION

Definitions and Syntheses of Consolidated Ligands with Different Topologies. Four different topological alignments of the binding sequences and the intervening linkers were assembled by solid-phase synthesis (Figure 1). The branched orientation of the type A ligands was achieved as reported previously (*19*), and the linear orientations of the type C and D ligands were achieved by straightforward stepwise Fmoc syntheses. To obtain the type B ligands, which have the N-termini of the two binding sequences in close proximity, a new strategy was developed. Starting with Fmoc-PAL-PEG-PS, we built the 2BP-1 (SH2-binding peptide) sequence and the oligoglycyl spacer in the C → N direction. The free amine was acylated with glutaric anhydride, and the pendant ω-carboxyl was activated in situ and coupled with the 3BP-2

(SH3-binding segment) amide sequence (PPAYPPPPVP) (2 equiv) that had been made separately on Fmoc-PAL-PEG-PS, cleaved, and purified. Corresponding experiments with succinic anhydride gave unacceptably low coupling yields, most likely due to succinimide formation upon activation of the pendant carboxyl. Among numerous protocols examined, the best yields were achieved upon activation with HATU/HOAt/NMM (2:2:4, with respect to peptide resin). The members of all four peptide ligand families were released from the solid supports by treatment with reagent K (35:2:2:2:1 TFA/phenol/H_2O/thioanisole/1,2-ethanedithiol) (*20*), purified by reversed-phase HPLC, and characterized by ESMS. Overall isolated yields were 20−40%, and materials that were assayed were ≥93% pure.

In Figure 4, the crystal structures of the SH2 of the SH(32) segments of Abl, Lck, Grb2, Src, and Hck are superimposed, on the basis of a backbone alignment of their SH2 domains (panel A). The complete topological set of ligands for the Abl SH(32) dual domains are illustrated in Figure 2, along with the binding affinities of synthesized members of each family. The linkers connecting the domains are adjusted in length so that the two ligands are spaced and oriented for optimal affinity for the target protein. The linkers here are comprised of glycyl residues, and five to eight glycyls were found to be optimal for types A and C.

Both type A and type C ligands bind to SH2 and SH3 subdomains in SH(32) with high specificities and affinities ($K_d \sim 200$ nM). A one order of magnitude increase was observed with respect to the most strongly bound single ligand (2BP-1, $K_d = 2350$ nM), and an increase of approximately 2 orders of magnitude was observed compared to those of low-affinity ligands (types B and D) which bind only with SH2 domains, as shown by competitive inhibition studies with ligands to SH2 or SH3; e.g., the bindings of 3BP-2 to SH(32) have similar constants ($K_d \sim 10$ μM) in the presence and absence of type D ligands. The values of affinities of ligands with variable linker lengths are most readily interpreted as indicating an optimal length of about G_6 (type A ligands) or G_7 (type C ligands), with little interaction between the linker and the SH(32) protein. The ability of SH(32) to bind to two alternate topologies presumably reflects the flexibility of the peptide segment between SH3 and SH2; i.e., the solution structure of the protein can convert between states binding tightly to topologies A and C.

Formation of a 1:1 Complex. The previous section invoked conformational interconversion and inherent flexibility to explain the tight binding of multiple topologies of the conformational ligands. An alternative explanation might be that the complexes formed are not truly 1:1 ligand−protein complexes but involve inter-multidomain self-association [e.g., in SH(32) molecule A, the SH3 is ligated to the consolidated ligand, while the same ligand binds to the SH2 of molecule B of SH(32)]. If this was so, then one would predict a strong dependence on the protein concentration of the apparent bimolecular affinity which would be due to formation of a ternary complex. The fluorimetry assay was carried out over a narrow range of protein concentrations, but no dependence on concentration was observed. Using isothermal titration calorimetry (Figure 5), the apparent K_d for the interaction of the type A ligand with the Abl SH(32) protein was ∼400 nM, inconsistent with the formation of a ternary complex, but indicative of the possibility of a slightly reduced affinity from dependence on SH(32) protein concentration. It may be concluded that the principal interaction of the SH(32) with the consolidated ligands is the formation of a 1:1 complex. The rotational correlation times for free and ligated forms are also inconsistent with a ternary complex (*25*).

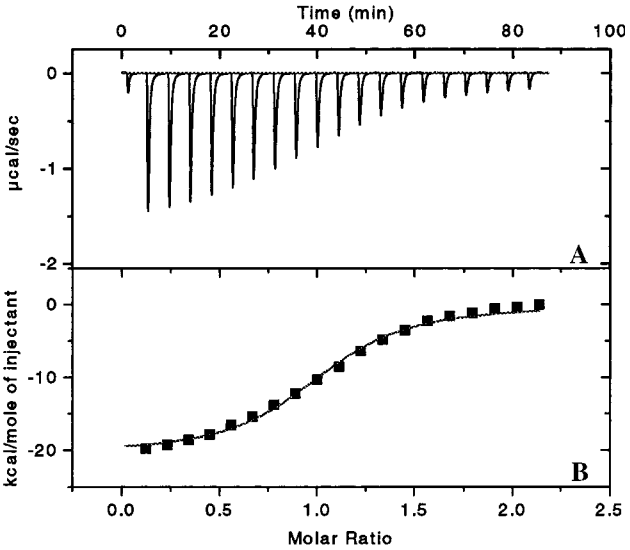

FIGURE 5: Ligand binding determined by isothermal titration microcalorimetry. (A) Trace of the calorimetric titration of Abl SH(32) (0.014 mM) with a type A ligand ($n = 6$, 0.34 mM) at 20 °C; details are in Materials and Methods. (B) Binding isotherm obtained from the experiment shown in panel A. The best fit to these data shows that the binding reaction is enthalpically (ΔH) driven and entropically (ΔS) unfavorable ($\Delta H = -20.6$ kcal/mol and $T\Delta S = -12.3$ kcal/mol; another run showed similar results, where $\Delta H = -19.0$ kcal/mol and $T\Delta S = -10.5$ kcal/mol). The value for K_D thus obtained was 430 nM (for another run, it was 450 nM). These measurements concluded that this binding involves the formation of a large number of contacts, which are enthalpically favorable, and a loss of conformational freedom upon binding is associated with a loss of entropy.

Can the Orientation of the Subligands Switch? An alternative hypothesis for the conformational interconversion might involve the ability of one of the subligands to bind in alternative structural modes. Since this is a known characteristic of some SH3 ligands (type I and type II binding; reviewed in ref *16*), this possibility needs close consideration. The alternative may be rejected for the following reasons. First, the ligands which have type I and II binding require the exchange of orientating groups [specifically positively charged residues for the Src case (*26*)] to provide the alternates. The ligands used here have a constant sequence for their SH3 binding segment, and this sequence is likely, from the crystal structure of the SH3−ligand complex (*22*), to involve specific orientating recognition at its N-terminus. Second, the specific peptide with the reverse sequence of 3BP-2 was made here, and shown to have an approximately millimolar binding affinity for Abl. It seems very unlikely that any counter orientation binding could then give rise to the high-affinity binding seen in topology series A or C. This is further supported by NMR titration data. $^1H\{^{15}N\}$ spectra were recorded for complexes, and spectra are illustrated in Figure 3. Direct structural and dynamic studies for investigating these complexes further are now in progress.

CONCLUSIONS

This work offers several new perspectives. First, in contrast to diffraction showing well defined relationships between SH2 and SH3 domains in SH(32)'s (reviewed in ref *12*) in Src kinases, the study described here, probing the orientation of Abl SH(32), and a related NMR study (*6*) definitely establish that the orientation of SH3 and SH2 domains in Abl SH(32) is not fixed, and can probably accommodate a wide range of relative orientations of the binding sites. This is potentially significant for the role of SH3 and SH2 domains in processive targeting in active kinases, and in the targeting of SH(32)-containing adapters. Clearly, the relative orientation between SH3 and SH2 plays an important role in the mediation of the activity of tyrosine kinases (*12*). For example (at least in the case of Src and Hck), in the inactive form, the SH3 and SH2 pack at the kinase domain which plays an inhibition role; while in the active form, SH3 and SH2 domains presumably move out and interact with other proteins which may play a role in localizing the kinases to the proper locations.

Second, the approach described here provides a synthetic alternative to one part of the "SAR (Structure Activity Relationship) by NMR" (*27*) approach by complementing the step for determining the structure of a ternary complex [equivalent to that of SH(32) with separate ligands to SH2 and SH3 subdomains]. The relative orientation and distance between subsites can be probed synthetically, as described here, and our approach is not limited to the molecular weight range of the NMR-based approach. Since the screening step of "SAR by NMR" is likely to be effective for significantly higher molecular weights than the structure-determining steps, the addition of topological synthesis of consolidated ligands may significantly extend the molecular weight range of strategies for efficiently discovering high-affinity ligands.

ACKNOWLEDGMENT

D.C. thanks Profs. Wayne Hendrickson and Bruce Mayer for discussion.

REFERENCES

1. Netzer, W. J., and Hartl, U. F. (1997) *Nature 388*, 343−349.
2. Cohen, G. B., Ren, R., and Baltimore, D. (1995) *Cell 80*, 237−248.
3. Cowburn, D., and Kuriyan, J. (1996) in *Signal Transduction* (Heldin, C.-H., and Purton, M., Eds.) pp 127−142, Chapman & Hall, London.
4. Pawson, T. (1995) *Nature 373*, 573−580.
5. Eck, M. J., Atwell, S. K., Shoelson, S. E., and Harrison, S. C. (1994) *Nature 368*, 764−769.
6. Gosser, Y. Q., Zheng, J., Overduin, M., Mayer, B. J., and Cowburn, D. (1995) *Structure 3*, 1075−1086.
7. Nam, H. J., Haser, W. G., Roberts, T. M., and Frederick, C. A. (1996) *Structure 4*, 1105−1114.
8. Sicheri, F., Moarefi, I., and Kuriyan, J. (1997) *Nature 385*, 602−609.
9. Xu, W., Harrison, S. C., and Eck, M. J. (1997) *Nature 385*, 595−602.
10. Williams, J. C., Weijland, A., Gonfloni, S., Thompson, A., Courtneidge, S. A., Superti-Furga, G., and Wierenga, R. K. (1997) *J. Mol. Biol. 274*, 757−775.
11. Cowburn, D., Zheng, J., Xu, Q., and Barany, G. (1995) *J. Biol. Chem. 270*, 26738−26741.
12. Sicheri, F., and Kuriyan, J. (1997) *Curr. Opin. Struct. Biol. 7*, 777−785.
13. Maignan, S., Guilloteau, J. P., Fromage, N., Arnoux, B., Becquart, J., and Ducruix, A. (1995) *Science 268*, 291−293.
14. Rosen, M. K., Yamazaki, T., Gish, G. D., Kay, C. M., Pawson, T., and Kay, L. E. (1995) *Nature 374*, 477−479.
15. Mayer, B. J., Hirai, H., and Sakai, R. (1995) *Curr. Biol. 5*, 296−305.
16. Kuriyan, J., and Cowburn, D. (1997) *Annu. Rev. Biophys. Biomol. Struct. 26*, 259−288.
17. Alberico, F., Kneib-Cordonier, N., Biancalana, S., Gera, L., Masada, R. L., Hudson, D., and Barany, G. (1990) *J. Org. Chem. 55*, 3730−3743.
18. Ottinger, E. A., Shekels, L. L., Bernlohr, D. A., and Barany, G. (1993) *Biochemistry 32*, 4354−4361.
19. Xu, Q., Cowburn, D., Zheng, J., and Barany, G. (1996) *Lett. Pept. Sci. 3*, 31−36.
20. King, D. S., Fields, C. G., and Fields, G. B. (1990) *Int. J. Pept. Protein Res. 36*, 225.
21. Overduin, M., Rios, C., Mayer, B., Baltimore, D., and Cowburn, D. (1992) *Cell 70*, 697−704.
22. Musacchio, A., Saraste, M., and Wilmanns, M. (1994) *Nat. Struct. Biol. 1*, 546−551.
23. Evans, S. V. (1993) *J. Mol. Graphics 11*, 134−138.
24. Wiseman, T., Williston, S., Brandts, J. F., and Lin, L. N. (1989) *Anal. Biochem. 179*, 131−137.
25. Fushman, D., Xu, R., and Cowburn, D. (1998) (submitted for publication).
26. Feng, S., Chen, J. K., Yu, H., Simon, J. A., and Schreiber, S. L. (1994) *Science 266*, 1241−1247.
27. Shuker, S. B., Hajduk, P. J., Meadows, R. P., and Fesik, S. W. (1996) *Science 274*, 1531−1534.

BI982744J